and that only a monotonic change would be seen in the exchange coupling constant. Whether J would increase or decrease with ϕ/r for such a series of complexes would depend largely on the identity of the lowest lying level. However, as Scaringe[1] has shown for the complexes under consideration here, the magnetic data clearly demonstrate that the difference $|E_2 - E_1|$ determines the observed trend in the exchange coupling.

Attempts to understand the exchange coupling mechanism and the magnitude of the singlet–triplet splitting must take into account both the bilinear exchange coupling constant from the term $-2JS_1 \cdot S_2$ and the biquadratic exchange coupling constant from the term $-2j(S_1 \cdot S_2)^2$. This latter term accounts for the departure of the energy levels from the interval rule given by $J[S'(S' + 1)]$ and results in a triplet–singlet splitting $|\Delta E|$ of $2J - 6.5j$. The singlet–triplet splittings, ΔE, from Table I are plotted as a function of ϕ/r in Figure 2. It may be seen in Figure 2 that the expected behavior of the singlet–triplet splitting is observed, that is, ΔE increases with an increase in ϕ/r, reaches a maximum at about 50°/Å and then decreases with a further increase in ϕ/r, although there is some scatter in the data. Presumably these minor variations from the overall trend arise from intermolecular interactions through hydrogen-bonding networks which differ widely in the set of complexes, from electronic effects that arise as a result of orbitals on nonbridging donor atoms, and from structural variations other than ϕ and r. Data on additional members of this series of hydroxo-bridged chromium(III) complex may permit an understanding of these secondary effects, but it is clear from these studies that the major structural factors affecting exchange coupling in these complexes are the angles at the bridging oxygen atom and the chromium(III)–oxygen bridge) bond distance. Furthermore, the experimental results may be described qualitatively by molecular orbital theory and these results provide considerable stimulation for quantitative calculations.

Acknowledgment. This research was supported by the National Science Foundation through research Grant No. CHE80 09685.

Registry No. $Cr_2(EDDA)_2(OH)_2$, 78340-40-6; Cr(EDDA)(acac), 26085-42-7.

Contribution from the Paul M. Gross Chemical Laboratory,
Duke University, Durham, North Carolina 27706

Hypersensitive Transition Probability in Tris(1,3-diphenyl-1,3-propanedionato)aquolanthanides(III)

ANDREW FULLER KIRBY and RICHARD ALAN PALMER*

Received January 16, 1981

Experimental oscillator strengths are found for f → f electronic transitions in solid-state tris(1,3-diphenyl-1,3-propanedionato)aquolanthanides(III) and used in the determination of Judd–Ofelt parameters. The dynamic coupling model is employed to predict the electric dipole intensity of certain hypersensitive transitions. Theoretical calculations concerning hypersensitivity are compared with experimental findings.

Introduction

In the last several years, there has been a considerable interest in the potential mechanism responsible for the anomolous intensity observed for certain f → f electronic transitions in lanthanides.[1-5] Recently, we have reported a detailed investigation of the ${}^4I_{9/2} \rightarrow {}^4G_{5/2}$ hypersensitive transition in solid-state tris(1,3-diphenyl-1,3-propanedionato)aquoneodymium(III) ($Nd(DBM)_3H_2O$) where theoretical calculations of oscillator strengh were carried out within the context of the dynamic coupling model proposed by Mason et al.[6] In this study, we wish to report a similar investigation of the hypersensitive transitions of europium (${}^7F_0 \rightarrow {}^5D_2$), holmium (${}^5I_8 \rightarrow {}^5G_6$), and erbium (${}^4I_{15/2} \rightarrow {}^4G_{11/2}$), in which the host is isomorphic with the neodymium analogue (see Table V).

In the dynamic coupling model, mutual perturbation of the metal ion and ligands results in a Coulombic correlation between transient-induced dipoles of the ligands and the quadrupole of the metal ion.[1] The extent of this coupling will be directly determined by the polarizability of the ligands. Specifically, this *theoretical* model predicts that the strength of the transition will be determined by eq 1, where Ω_2(dyn)

$$\Omega_2(\text{dyn}) = \frac{28}{5}\langle 4f|r^2|4f\rangle^2 \sum_{m=0}^{3}(2 - \delta_{m,o})|\sum \bar{\alpha}_{(L)} R_{(L)}{}^{-4} C_{-m}{}^{(3)}(L)|^2 \quad (1)$$

(dyn = dynamic), a transition strength parameter, is related to a sum of the product of $\bar{\alpha}_{(L)}$, the mean polarizability of the ligand, $R_{(L)}$, the metal–ligand bond distance, and $C_{-m}{}^{(3)}$, a third rank spherical tensor which is determined by the pertinent structural parameters. The radial expectation value of the f electron must also be calculated, as expressed by the $\langle 4f|r^2|4f\rangle$ radial integral.

On the other hand, a particularly useful means for ordering the *experimentally observed* oscillator strengths of all transitions in a lanthanide spectrum is afforded by the Judd–Ofelt equation.[7,8] The expression is given by eq 2, where P is the

$$P_{\text{ed}} = \chi\left[\frac{8\pi^2 mc}{3h}\right]\bar{\nu} \sum_{\lambda=2,4,6} \Omega_\lambda \langle f^n \| U^\lambda \| f^{n'}\rangle^2 (2J + 1)^{-1} \quad (2)$$

electric dipole oscillator strength of an f → f transition as expressed by the sum of the products of the Ω_λ parameters and the appropriate transition matrix elements at $\bar{\nu}$, the frequency of the transition, and corrected by χ, the Lorentz field factor, which is a function of the refractive index of the bulk medium. It is common practice to find a set of Ω_λ parameters by a

---

(1) Mason, S. F. *Struct. Bonding (Berlin)* **1980**, *39*, 43.
(2) Peacock, R. D. *Struct. Bonding (Berlin)* **1975**, *22*, 83.
(3) Henrie, D. E.; Fellows, R. L.; Choppin, G. R. *Coord. Chem. Rev.* **1976**, *18*, 199.
(4) Judd, B. R. *J. Chem. Phys.* **1978**, *70*, 4830.
(5) Karraker, D. G. *Inorg. Chem.* **1967**, *6*, 1863.
(6) Kirby, A. F.; Palmer, R. A. *Inorg. Chem.* **1981**, *20*, 1030.
(7) Judd, B. R. *Phys. Rev.* **1962**, *127*, 750.
(8) Ofelt, G. S. *J. Chem. Phys.* **1962**, *37*, 511.

0020-1669/81/1320-4219$01.25/0

least-squares analysis which suitably reproduces the experimentally observed intensities of all of the f → f transitions. Details concerning the derivation and use of this equation are found elsewhere.[2]

Because the magnitude of the $U^{(2)}$ matrix element is vanishingly small for "normal transitions", only Ω_4 and Ω_6 are important in the intensity calculation by eq 2. In contrast, for hypersensitive transitions it is clear that the most significant transition strength parameter is Ω_2. When $U^{(2)}$ is large (which is only true when $\Delta J \leq 2$), the Ω_2 parameter often accounts for most, if not all, of the calculated intensity. It is for this general case that eq 1 has been given in terms of Ω_2. Therefore, calculation of Ω_2 by eq 1 and determination of Ω_2 by eq 2 allow a direct comparison to be made between the experimentally observed hypersensitive transition intensity and its theoretically predicted value, which is based on structural and ligand polarizability data.

Solid-state tris(1,3-diphenyl-1,3-propanedionato)aquolanthanides(III) ($Ln(DBM)_3H_2O$) have a seven-coordinate structure best described as a three-bladed propeller capped by a single water molecule on the threefold axis. The metal ion has C_3 site symmetry with its rotation axis parallel to the unique axis of the enantiomorphic R3 crystal. The high symmetry and well-defined coordination sphere of these compounds make them particularly suitable for electronic absorption studies. In addition, detailed structural information is available for both the neodymium and holmium analogues.[6,9]

Experimental Section

Preparation of Tris(1,3-diphenyl-1,3-propanedionato)aquolanthanide(III) Compounds. The dry rare-earth perchlorates were obtained by dissolution of the corresponding oxides M_2O_3 in a stochiometric amount of 30% perchloric acid, followed by gentle heating to remove excess water. Twelve millimoles of dibenzoylmethane was added to a solution of 100 mL of spectral-grade acetone and 25 mL of 0.5 M KOH. Four millimoles of the appropriate rare-earth perchlorate was dissolved in 20 mL of water; this mixture was then added dropwise while stirring to the ligand solution at room temperature. The complex solution was carefully filtered through Celite, and crystals were allowed to grow by slow evaporation. Single crystals of suitable size for spectroscopic study were obtained for holmium and europium, but only microcrystals could be prepared for erbium by this method of crystallization.

Instrumentation. All absorption measurements were made at 295 and 77 K with the use of a Cary 14R spectrometer in the visible mode. Single-crystal spectra were obtained orthoaxially by using incident radiation which was plane polarized by a Glan–Thompson quartz prism. Spectra of mulled samples were obtained by suspending finely powdered samples in Nujol and pressing the mull to suitable thickness between small quartz plates.

Experimental and Theoretical Oscillator Strengths. Spectra were collected for several different thicknesses of both single crystals and mulls. Crystal thickness was determined with a microscope stage micrometer, and concentration was then calculated from the crystallographic data. Molar absorptivities of bands in the mull spectra were determined by scaling the relative integrated intensities observed in the mull to those observed in the single crystal. In the case of $Er(DBM)_3H_2O$, where single-crystal data could not be obtained, a mixed mull was prepared of the erbium and holmium compounds; the integrated intensities of the f → f transitions in an $Er(DBM)_3H_2O$ mull could then be scaled to the $Ho(DBM)_3H_2O$ single-crystal spectra.

Integrated band intensities for those transitions observed were determined by eq 3 where ϵ is the molar absorptivity at energy $\bar{\nu}$. When

$$I = \int (\epsilon/\bar{\nu})\, d\bar{\nu} \approx (1/\bar{\nu}_{max}) \int \epsilon\, d\bar{\nu} \qquad (3)$$

orthoaxial single-crystal spectra were obtained, the isotropic integrated intensity was calculated by eq 4 where $I_\perp$ and $I_\parallel$ are the intensities

$$\langle I_{iso} \rangle = {}^2\!/_3 I_\perp + {}^1\!/_3 I_\parallel \qquad (4)$$

observed for the perpendicular and parallel polarizations. The final experimental oscillator strengths were obtained from eq 5. So that

$$P_{exptl} = 4.318 \times 10^{-9} \int \epsilon_{\bar{\nu}}\, d\bar{\nu} \qquad (5)$$

the Ω_λ parameters of eq 2 could be calculated, the Lorentz field correction, χ, was calculated from eq 6 where the refractive index

$$\chi = (n^2 + 2)^2/9n \qquad (6)$$

is a function of the simple Cauchy relation eq 7.

$$n(\lambda) = A + B/\lambda^2 + C/\lambda^4 + \ldots \qquad (7)$$

Table I. Measured and Calculated *P* for $Ho(DBM)_3H_2O$

$[S',L']J'$	E,[a] cm^{-1}	$10^6 P_{exptl}$	$10^6 P_{calcd}$[b]
$^5F_5$	15 000	1.1	1.7
$^5S_2$ $^5F_4$	18 000	3.4	3.5
$^5F_3$	20 600	1.8	1.5
$^5F_2$	21 100	0.9	0.9
$^3K_8$	21 400	4.0	2.8
$^5G_6$	22 100	158	158
$^5G_5$	23 950	62[a]	<1

[a] Transition could not be used in this calculation. [b] Rms = 5.7×10^{-7}.

Table II. Measured and Calculated *P* for $Er(DBM)_3H_2O$

$[S',L']J'$	E, cm^{-1}	$10^6 P_{exptl}$	$10^6 P_{calcd}$[a]
$^4F_{9/2}$	15 300	5.6	6.0
$^4S_{3/2}$	18 400	3.6	3.0
$^2H_{11/2}$	19 200	60	60
$^4F_{7/2}$	20 500	11	10
$^4F_{5/2}$ $^4F_{3/2}$	22 400	4.6	6.1

[a] Rms = 8.5×10^{-7}.

Table III. Measured *P* for $Eu(DBM)_3H_2O$

$[S',L']J'$	E, cm^{-1}	$10^6 P_{exptl}$	$[S',L']J'$	E, cm^{-1}	$10^6 P_{exptl}$
$^5D_2$	21 460	2.45	$^5D_0$	17 240	<0.1
$^5D_1$	17 240	<0.1			

For calculation of Ω_2 by eq 1, polarizabilities were obtained according to the methods of Miller et al.[11] the radial integrals used were those of Freeman and Watson,[12] and the structural parameters were estimated from the published crystal structures of $Nd(DBM)_3H_2O$ and $Ho(DBM)_3H_2O$ in accordance with the radius expected by interpolation for each isomorphic chromophore.[6,9]

Results

Electronic absorption spectra were obtained for $Ln(DBM)_3H_2O$ (where Ln = Eu, Ho, and Er) at room temperature and at 77 K. Single-crystal measurements were made orthoaxially for europium and holmium, while for erbium it was necessary to use mulled microcrystals. Only the transitions as assigned and listed in Tables I and II were used in the determination of the experimentally adjusted Judd–Ofelt parameters for solid-state $Ho(DBM)_3H_2O$ and $Er(DBM)_3H_2O$. Judd–Ofelt parameters were not calculated for $Eu(DBM)_3H_2O$ as only three f → f transitions from the ground state could be observed; these are listed in Table III. The connecting matrix elements as calculated by Carnall et al. were used in the determination of Ω_2, Ω_4, and Ω_6 of eq 2.[13,14] The Cauchy constants used for the refractive index and Lorentz field correction were those calculated in a previous study.[6] All experimental intensities reported in this work reflect an isotropic orientation of the sample. Detailed analysis of the crystal field splittings observed in the europium compound has

---

(9) Zalkin, A.; Templeton, D. H.; Karraker, D. G. *Inorg. Chem.* **1969**, *8*, 2680.

(10) Lomheim, T. S.; DeShazer, L. G. *J. Appl. Phys.* **1978**, *49*, 5517.

(11) Miller, K. J.; Savchik, J. A. *J. Chem. Soc.* **1979**, *101*, 7206.

(12) Freeman, A. J.; Watson, R. E. *Phys. Rev.* **1962**, *127*, 2058.

(13) Carnall, W. T.; Fields, P. R.; Rajnak, K. *J. Chem. Phys.* **1968**, *49*, 4450.

(14) Carnall, W. T.; Fields, P. R.; Rajnak, K. *J. Chem. Phys.* **1968**, *49*, 4424.

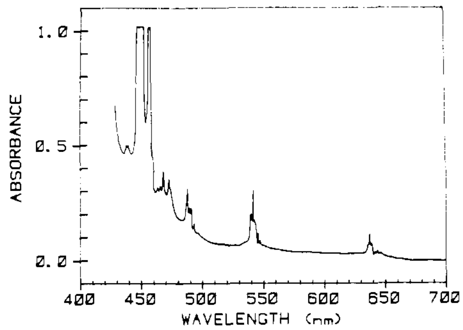

Figure 1. Single-crystal orthoaxial absorption spectrum of Ho-$(DBM)_3H_2O$; π polarization, $T = 77$ K.

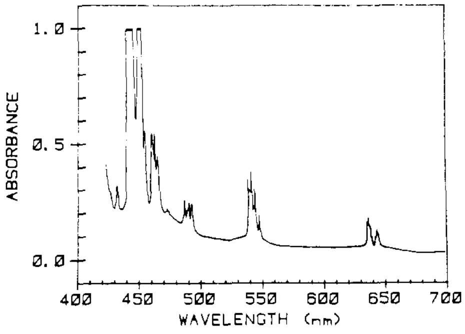

Figure 2. Single-crystal orthoaxial absorption spectrum of Ho-$(DBM)_3H_2O$; σ polarization, $T = 77$ K.

Table IV. Ω_λ Parameters for Solid-State $Ln(DBM)_3H_2O$[a]

Ln	Ω_2(dyn)[b]	Ω_2(J-O)[c]	Ω_4(J-O)	Ω_6(J-O)
Nd^{3+}	56.6	44.7	11.9	1.25
Eu^{3+}	44.6	78.8		
Ho^{3+}	35.4	42.8	<0.01	1.95
Er^{3+}	33.5	35.1	1.11	6.64

[a] All parameters are in units of 10^{-20} cm². [b] Calculated from dynamic coupling model. [c] Obtained from Judd-Ofelt equation experimentally.

appeared in another communication.[15]

$Ho(DBM)_3H_2O$ (f^{10}). Transitions were observed from the $^5I_8$ ground state to the $^5F_5$, $^5S_2$, $^5F_4$, $^5F_3$, $^5F_2$, $^3K_8$, $^5G_6$, and $^5G_5$ exited states. The single-crystal spectra are shown in Figures 1 and 2. Reliable Judd-Ofelt parameters could be obtained from the integrated intensities only if no attempt was made to calculate the intensities of the $^5I_8 \rightarrow {}^5G_6$ and $^5I_8 \rightarrow {}^5G_5$ transitions simultaneously. The final Judd-Ofelt parameters obtained are listed in Table IV. In this case, the experimental value of Ω_2 is principally a reflection of the intensity of the $^5I_8 \rightarrow {}^5G_6$ hypersensitive transition.

$Er(DBM)_3H_2O$ (f^{11}). In this system, transitions were observed from the $^4I_{15/2}$ ground state to the $^4F_{9/2}$, $^4S_{3/2}$, $^2H_{11/2}$, $^4F_{7/2}$, $^4F_{5/2}$, and $^4F_{3/2}$ exited states. Satisfactory precision was achieved in the determination of Ω_2, Ω_4, and Ω_6 when all observed transitions were used in the least-squares calculation; the final parameters are listed in Table IV. It was not necessary to generate the integrated intensities expected for an isotropic (or random) orientation as this is already assumed to be the case in the mull spectrum, as presented in Figure 3.

$Eu(DBM)_3H_2O$ (f^6). Only transitions from the nondegenerate $^7F_0$ ground state to the $^5D_0$, $^5D_1$, and $^5D_2$ excited states could be observed in the 77 K spectrum (Figure 4). At room temperature, additional transitions appear from the thermally populated $^7F_1$ level to the $^5D_1$ and $^5D_2$ states. Many of these transitions are formally forbidden by the pure electric dipole selection rules; hence no attempt was made here to establish the experimental parameters Ω_4 and Ω_6 (see Table V). However, the $^7F_0 \rightarrow {}^5D_2$ hypersensitive transition has a nonzero $U^{(2)}$ matrix element, which makes it possible to solve exclusively for the Ω_2 parameter. Consequently, the experimental Ω_2 reported in Table IV is dependent solely on the observed intensity of a single transition and has been calculated for the purpose of comparison.

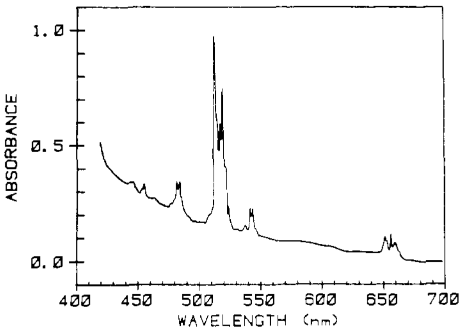

Figure 3. Mulled microcrystal absorption spectrum of $Er(DBM)_3H_2O$; $T = 77$ K.

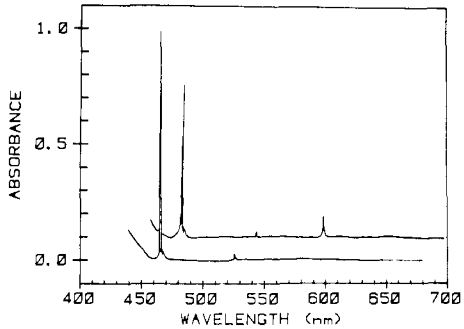

Figure 4. Single-crystal orthoaxial absorption spectrum of Eu-$(DBM)_3H_2O$ ($T = 77$ K): upper offset trace is π polarization; lower trace, σ polarization.

Table V. Hypersensitive Transitions[a] in $Ln(DBM)_3H_2O$

Ln	transition	E, cm⁻¹	$10^6 \times P_{DBM}$	$10^6 \times P_{aquo}$
Nd^{3+}	$^4I_{9/2} \rightarrow {}^4G_{5/2}$	17 050	150	9.8
Eu^{3+}	$^7F_0 \rightarrow {}^5D_2$	21 460	2.54	0.01
Ho^{3+}	$^5I_8 \rightarrow {}^5G_6$	22 170	158	6.0
Er^{3+}	$^4I_{15/2} \rightarrow {}^2H_{11/2}$	19 140	55.9	2.9

[a] Selection rules: electric quadrupole, $|\Delta L| \leq 2$ and $|\Delta J| \leq 2$; electric dipole, $|\Delta L| \leq 6$ and $|\Delta J| \leq 6$, but not $0 \nleftrightarrow 1, 3, 5$; magnetic dipole, $\Delta L = 0$; $\Delta J = \pm 1, 0$; but not $0 \nleftrightarrow 0$; spin, $\Delta S = 0$.

Theoretical Calculations. The $\langle 4f|r^2|4f\rangle$ radial integrals needed for calculation of Ω_2 by eq 1 were obtained directly from the work of Freeman and Watson.[12] The average molecular polarizabilities used were, of course, the same for each isomorph and were determined by a convenient method recently reported by Miller and Savchik.[11] The structural data required for each calculation were either obtained directly from the published structures of $Nd(DBM)_3H_2O$ and Ho-$(DBM)_3H_2O$ or interpolated or extrapolated in accordance with the expected ionic radii. The results for calculation of Ω_2 by the dynamic coupling model for the europium, holmium, and erbium compounds are given in Table IV and, in addition, a value for the neodymium compound is listed for comparison.

Discussion

Much of the interest in the phenomenon of hypersensitivity has centered about an effort to implicate a particular intensity

---

(15) Kirby, A. F.; Palmer, R. A. *Chem. Phys. Lett.* **1980**, *80*, 142.

promoting mechanism. Apart from certain symmetry requirements (i.e., those concerning electric dipole selection rules), some of the effects which have been considered include covalency, ligand basicity, the nephelauxetic effect, solvent properties, and ligand polarizability.[2] The study of the hypersensitivity of several Ln^{3+} chromophores within an isomorphous series affords an opportunity to maintain a constant chemical environment about the metal ion. This is especially true in the solid state, where only the metal to ligand bond distance changes across the series and the potential rearrangements of the structure due to the lability of the Ln^{3+} ion need not be considered.

Part of the motivation for this study was to determine if the smooth trend predicted by eq 1 for the variation of the Ω_2 transition strength parameter across the Ln^{3+} series could be observed experimentally, especially in the $Ln(DBM)_3H_2O$ system where hypersensitivity is such an important phenomenon. The dynamic coupling model clearly implies, all other factors being equal (including polarizability in this case), that only changes in the ligand–metal distance and the radial integral value can effect a change in Ω_2. As shown in Table IV, Ω_2 is theoretically predicted to be smallest for erbium and largest for neodymium, of the chromophores studied.

Experimentally, obtaining Ω_2 via eq 2 is not always a straightforward matter. In the case of $Ho(DBM)_3H_2O$, the $^5I_8 \rightarrow {}^5G_6$ transition is very intense, and the $^5I_8 \rightarrow {}^5G_5$ transition, which is not formally a hypersensitive transition, is also unusually intense (see Table I). However, the $U^{(2)}$ matrix element for the $^5I_8 \rightarrow {}^5G_5$ transition is 0. This makes rationalizing the intensities of other normal transitions difficult without anomalously increasing Ω_4 and Ω_6 for eq 2. For this reason, the latter transition was not used to establish the Judd–Ofelt parameters and consequently they are reliable only for Ω_2.

Analysis of the f → f transition intensities by eq 2 for $Er(DBM)_3H_2O$ is perfectly feasible for the transitions observed. However, due to the strong absorption of the ligand, which tails well into the visible, only the $^4I_{15/2} \rightarrow {}^2H_{11/2}$ hypersensitive transition at ca. 19 200 cm^{-1} was observed, while the predictably more intense $^4I_{15/2} \rightarrow {}^4G_{11/2}$ hypersensitive transition at ca. 26 400 cm^{-1} was obscured. It is difficult to speculate as to whether the same complication might have occurred as did in our previous work with $Nd(DBM)_3H_2O$, where two hypersensitive transitions could be observed ($^4I_{9/2} \rightarrow {}^4G_{5/2}$ at ca. 17 050 cm^{-1} and $^4I_{9/2} \rightarrow {}^4G_{7/2}$ at ca. 18 800 cm^{-1}) but were not easily rationalized by the same Ω_2 parameter.[6]

The $Eu(DBM)_3H_2O$ spectrum (Figure 4) is particularly interesting. The only f → f transition observed at 77 K between 6000 and 23 000 cm^{-1} which is allowed by the electric dipole mechanism of eq 2 is the $^7F_0 \rightarrow {}^5D_2$ hypersensitive transition at ca. 21 460 cm^{-1}. Although the $^7F_0 \rightarrow {}^5D_1$ transition is observed, it is presumed to gain its intensity via a magnetic dipole mechanism, an assumption for which there is ample precedent.[2] The $^7F_0 \rightarrow {}^5D_0$ transition is both electric and magnetic dipole forbidden and is predicted to have zero intensity. In a previous communication we concluded that the transition arises as a result of mixing between the $^7F_0$ and $^7F_2$ states, which would explain its apparent electric dipole character.[15] However, the $^7F_0 \rightarrow {}^5D_2$ hypersensitive transition indeed does have a nonzero $U^{(2)}$ matrix element ($U^{(4)}$ and $U^{(6)}$ are 0), making it possible to establish an experimental value for Ω_2 via eq 2, which depends only on the observed intensity of this one transition. The results of the experimental determination of Ω_2 given in Table IV show that, while a smooth trend is not followed, Ω_2 values for holmium, neodymium, and erbium are all very close (within the experimental error related to measurement of crystal thickness). $Eu(DBM)_3H_2O$, however, has an experimental Ω_2 which reflects a hypersensitive transition oscillator strength much greater than that predicted by the dynamic coupling model. We are currently making a more detailed investigation of the behavior of the europium species.

In conclusion, the experimental parameters most important in rationalizing the intensity of certain hypersensitive transitions in the $Ln(DBM)_3H_2O$ series (see Table V) do not vary smoothly as predicted by the dynamic coupling model. Yet, the magnitudes of Ω_2 calculated by eq 1 are remarkable in that they are at worst within 40% of the experimentally determined values from integrated intensities, values which vary by almost 2 orders of magnitude. Furthermore, the oscillator strengths of these transitions are still 1–2 orders of magnitude greater in the $Ln(DBM)_3H_2O$ system than they are in the Ln^{3+} aquated cations,[16] which are traditionally referenced for comparison.

Registry No. $Ho(DBM)_3H_2O$, 26202-50-6; $Er(DBM)_3H_2O$, 17168-64-8; $Eu(DBM)_3H_2O$, 12121-06-1.

---

(16) Reisfeld, R.; Jorgensen, C. K. "Lasers and Excited States of Rare Earths"; Springer-Verlag: Berlin 1977; p 138.